Chemistry, Geometry, and Defects in Two Dimensions

David J. Wales*

Department of Chemistry, University of Cambridge, Lensfield Road, Cambridge CB2 1EW, United Kingdom

ABSTRACT Particles restricted to spherical or curved surfaces can produce materials that behave very differently from analogues that are essentially flat. In particular, the appearance of defects can change the mechanical and optoelectrical properties. The length scales involved range from atomistic to mesoscopic and present an exciting frontier of research for both experiment and theory in molecular, materials, and soft matter science.

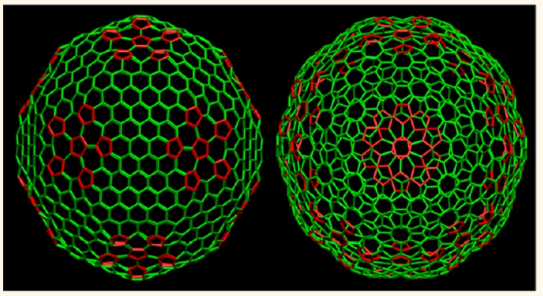

When J.J. Thomson proposed his model for atomic structure in 1904 in terms of unit charges constrained to the surface of a sphere,[1] he could not have envisaged its widespread application to diverse areas of materials, condensed matter, and molecular science. The "Thomson problem" for N charges is now generally understood as prediction of the lowest energy configuration for the potential $\sum_{i<j\leq N} 1/|r_i - r_j|$, with $|r_i| = 1$ for all particles i and j. Defects are an unavoidable consequence of geometry for spherical topology, and the appearance of various classes of defects for the Thomson problem, which are realized experimentally in systems spanning fullerenes, viruses, colloidal silica microspheres, superconducting films, and lipid rafts on vesicles, has sparked continued interest in this model. The insight gained from such predictions is especially important for mesoscopic systems, where atomistic descriptions lie beyond current computational capabilities, especially in view of the likely dependence of key mechanical, optical, and electrical properties on defect structure and dynamics.[2,3]

In this issue of *ACS Nano*, Sanjuan *et al.* report on connections between two-dimensional geometry and chemical properties, such as bond lengths and hybridization.[4] In particular, for carbon-based materials, they show that the pyramidalization angle is directly proportional to the mean curvature. This atomistic viewpoint adds details that are not included in more coarse-grained continuum models, which will be important for predicting and understanding chemical reactivity. For example, calculations for H_2 on graphene suggest that compression of the substrate can change endothermic dissociation of physisorbed H_2 to an exothermic process, lowering the barrier from 3.0 to 0.5 eV.[5] This chemisorption is predicted to cause significant strain in the substrate, lowering the barrier for further chemisorption. Such effects, and the systematic differences that are likely to arise for curved substrates, have important implications for hydrogen storage in carbon-based materials, as well as properties such as aromaticity.[6]

In this issue of *ACS Nano*, Sanjuan *et al.* report on connections between two-dimensional geometry and chemical properties, such as bond lengths and hybridization.

* Address correspondence to dw34@cam.ac.uk.

Published online February 13, 2014
10.1021/nn500645r

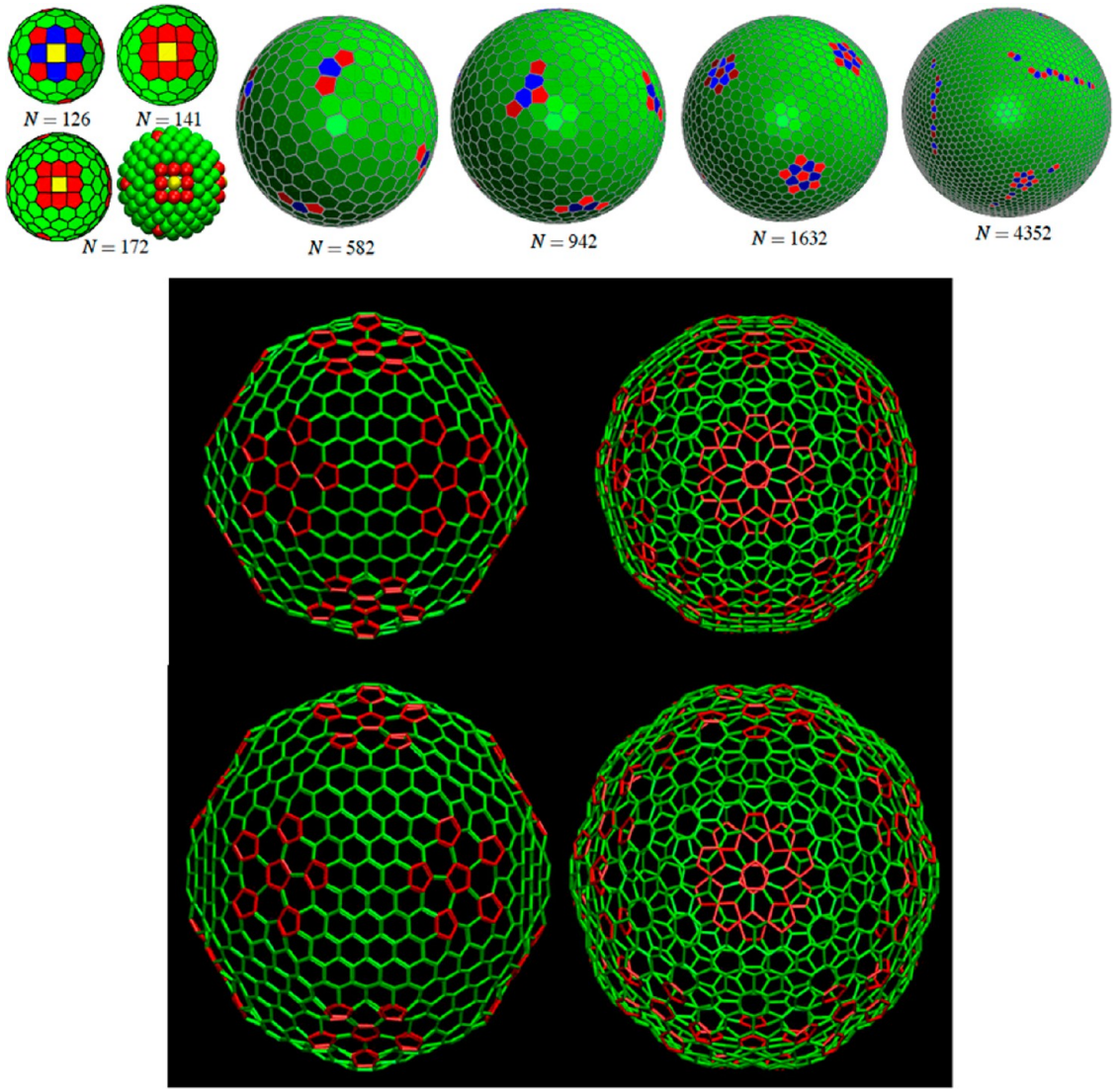

Figure 1. (Top) Evolution of defect structures predicted for global potential minima of the Thomson function as a function of size:[8,9] pentagon patches, extended dislocations (scars), twinned defects, rosettes, and embryonic grain boundaries. Voronoi constructions reflecting the number of nearest neighbors are shown for each size and compared with a representation based on particles for $N = 172$. (Bottom) Geometry-optimized C_{860} (top) and C_{1160} (bottom) clusters. Views are shown down the approximate C_2 (left) and C_5 (right) axes, with pentagonal rings highlighted in red.[8]

The defect structures predicted for the Thomson problem have already prompted analysis of carbon-based analogues, obtained by associating a carbon atom with each face of a triangulated structure.[7,8] The evolution of the favored defects with size is illustrated in Figure 1,[8,9] using a Voronoi construction where pentagons, hexagons, and heptagons correspond to particles with five, six, and seven neighbors. Icosahedral local minima were obtained for C_{860} and C_{1160} by relaxing structures corresponding to the lowest known minima of the Thomson potential (Figure 1).[8]

More generally, curved surfaces can produce competition between local order and geometrical constraints, and defects corresponding to 5-fold and 7-fold coordination are identified as disclinations with positive and negative topological charges, respectively. Neighboring particles with pentagonal and heptagonal coordination produce lines of dislocations, corresponding to pleats (*e.g.*, pentagon−heptagon dipoles) and scars[10] (*e.g.*, pentagon−heptagon−pentagon arrangements).

The product of the maximum and minimum curvatures, k_1 and k_2, of a surface projected onto planes containing the normal vector at any given point defines the Gaussian curvature, K, at that point. Disclinations should become favorable when the magnitude of K is sufficiently large and are realized for colloidal particles embedded in the interface corresponding to a capillary bridge.[11] The structures observed are in good agreement with theory for rigid surfaces with constant mean curvature $H = (k_1 + k_2)/2$, including catenoids ($H = 0$) and unduloids and nodoids (H constant but nonzero).[12,13] Some of the results for unduloid surfaces are illustrated in

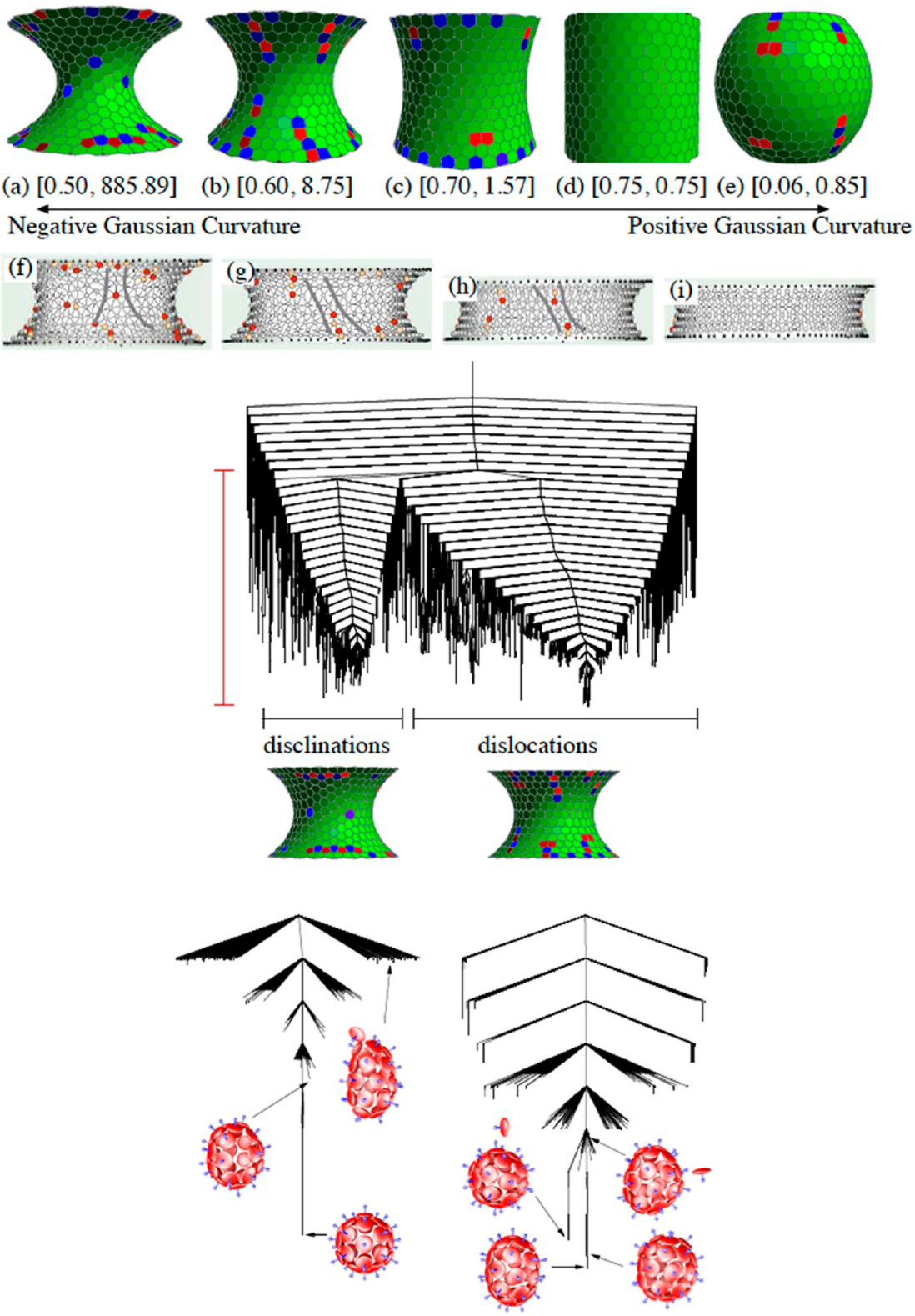

Figure 2. (Top) Defect motifs for unduloid surfaces with nonzero constant mean curvature. (a−e) Curvature of the capillary bridge is varied while keeping the height and volume constant. The corresponding values for the unduloid parameters [a,c] are given in square brackets. (f−i) Comparisons to experimental results of Irvine *et al.* for colloidal crystals,[11] where red particles have seven neighbors and yellow particles have five. Reproduced with permission from ref 12. Copyright 2013 American Physical Society. (Center) This disconnectivity graph illustrates the hierarchical structure and two representative local minima for a potential energy landscape corresponding to 600 particles embedded on a catenoid. The barrier between the two main funnels involved in interconverting different defect motifs is significantly larger than the barriers within the funnels for rearrangements of related defect structures. (Bottom) Disconnectivity graph for (left) 32 and (right) 33 unconstrained discoidal particles on the same vertical energy scale, with selected low-lying minima.[16]

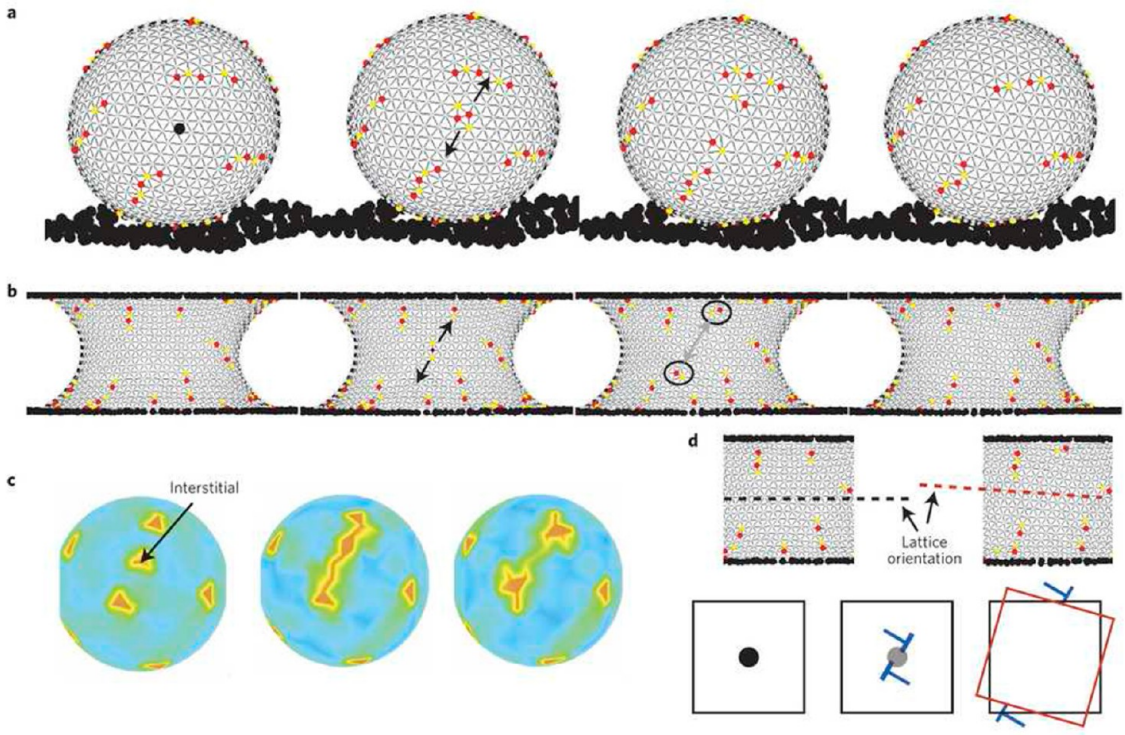

Figure 3. (a) Insertion of an interstitial in a spherical crystal is followed by its fissioning into two dislocations that migrate, gliding along parallel Bragg planes in opposite directions, and are subsequently absorbed into existing grain boundary scars. (b) Insertion of an interstitial (black-purple dot, representing an initially four-fold-coordinated defect, surrounded by two seven-fold-coordinated defects) on a negatively curved capillary bridge followed by its fissioning into two dislocations—the upper dislocation is absorbed by an existing dislocation that rotates to absorb the Burgers' vector, and the bottom dislocation is absorbed by an existing grain boundary scar. (c) Plot of the compressional strain distribution that accompanies a fractionalization event as evaluated numerically on a sphere. (d) Twisting of Bragg rows resulting from interstitial fractionalization as deduced from imaged configurations before and after fractionalization. The schematic illustrates the twisting of the crystalline patch (square) containing an interstitial as its constituent dislocations (blue nails) separate to globally distinct locations on the lattice. Reproduced with permission from ref 18. Copyright 2012 Nature Publishing Group.

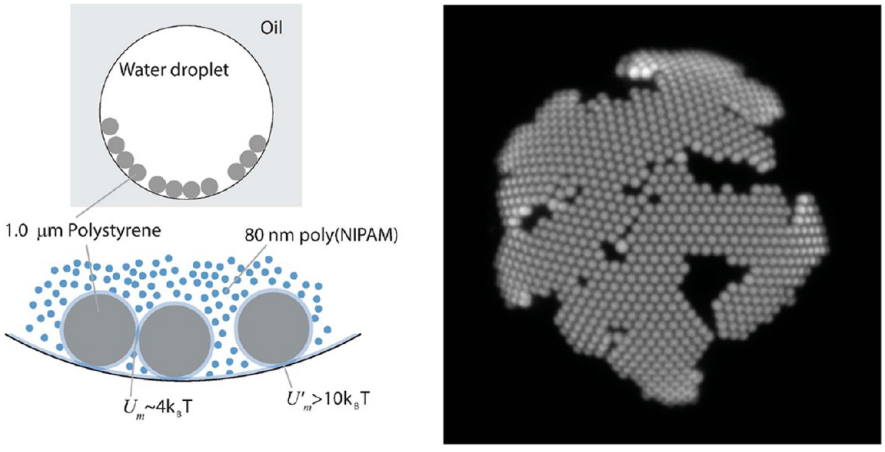

Figure 4. Rigid colloidal crystals form on the interior surfaces of spherical water-in-oil droplets encapsulating 1 mm polystyrene spheres and 80 nm poly(*N*-isopropylacrylamide) particles, which induce depletion attractions between the large spheres with a strength of about $4k_BT$, where k_BT is the thermal energy. The depletion interaction between the particles and the droplets is about $10k_BT$. The range of attraction is about 80 nm. A representative confocal fluorescence micrograph (right) shows a crystal grown for a few hours on a droplet of radius about 25 mm in diameter.

Figure 2. Visualizing the corresponding potential energy landscape using disconnectivity graphs[14,15] can also be insightful. For example, the landscape illustrated in Figure 2 reveals a double funnel structure defined by local minima with predominantly disclinations or dislocations.[12] For comparison, the effect of defects on the self-assembly of unconstrained discoidal particles can be seen in the disconnectivity graphs

for 32 and 33 particles in the bottom panel of Figure 2.[16] The global minimum for 32 discoids has icosahedral symmetry and a well-defined single potential energy funnel, associated with efficient self-organization.[17] In contrast, when an additional particle must be accommodated, a double funnel organization results, with a relatively flexible prolate global minimum separated from structures containing a single loosely bound particle by larger barriers.[16] Such systems are likely to exhibit polymorphism, and incorporating additional particles into shells corresponding to single funnels with more symmetrical global minima is likely to be kinetically unfavorable.

New experiments promise further insight into such dynamical behavior. For example, using optical tweezers and three-dimensional imaging, it has recently been possible to insert interstitial colloidal particles into flat and curved oil/glycerol interfaces.[18] Colloidal assemblies on curved surfaces were found to behave quite differently from flat surfaces, self-healing through remarkable collective particle reorganization. The results have been interpreted in terms of "particle fractionalization", where five- and seven-coordinate defects move apart independently (Figure 3).

The dramatic effect of curvature on crystal growth has also been visualized for two-dimensional colloidal crystals growing on spherical droplets.[19] In these experiments, the two-dimensional crystals grow on the interior surface of spherical water-in-oil droplets, driven by short-range depletion interactions. The structures are determined using confocal fluorescence microscopy and exhibit large single-crystal domains without topological defects (Figure 4). The domains exhibit high perimeter-to-area ratios, which arise from elastic stress rather than kinetic instabilities.[19] The experimental setup includes surfactant to prevent the particles from breaching the interface, so there are no capillary forces. In contrast, in the absence of surfactant, spherical colloids confined to a curved, anisotropic surface interact through quadrupolar capillary interactions,[20] leading to regular square lattices.

The ability to follow structure and non-equilibrium dynamics through direct imaging experiments such as these holds tremendous promise for the development of rational design principles in future work, through feedback between theory and experiment. For example, comparison of the favored morphologies that arise for alternative attractive or repulsive forces between confined particles has yet to be fully explored.

Conflict of Interest: The authors declare no competing financial interest.

Acknowledgment. D.J.W. gratefully acknowledges funding from the EPSRC and the ERC, helpful comments from Dr. H. Kusumaatmaja and Prof. M. Bowick, and Prof. V. Manoharan for supplying the source for Figure 4.

REFERENCES AND NOTES

1. Thomson, J. J. On the Structure of the Atom. *Philos. Mag.* **1904**, *7*, 237–265.
2. Nelson, D. R. *Defects and Geometry in Condensed Matter Physics*; Cambridge University Press: Cambridge, UK, 2002.
3. Lord, E. A.; Mackay, A. L.; Ranganathan, S. *New Geometries for New Materials*; Cambridge University Press: Cambridge, UK, 2006.
4. Pacheco Sanjuan, A. A.; Mehboudi, M.; Harriss, E. O.; Terrones, H.; Barraza-Lopez, S. Quantitative Chemistry and the Discrete Geometry of Conformal Atom-Thin Crystals. *ACS Nano* **2014**, DOI: 10.1021/nn406532z.
5. McKay, H.; Wales, D. J.; Jenkins, S. J.; Verges, J. A.; de Andres, P. L. Hydrogen on Graphene under Stress: Molecular Dissociation and Gap Opening. *Phys. Rev. B* **2010**, *81*, 075425.
6. Steiner, E.; Fowler, P. W. Ring Currents in Aromatic Hydrocarbons. *Int. J. Quantum Chem.* **1996**, *60*, 609–616.
7. Pérez-Garrido, A. Giant Multilayer Fullerene Structures with Symmetrically Arranged Defects. *Phys. Rev. B* **2000**, *62*, 6979–6981.
8. Wales, D. J.; McKay, H.; Altschuler, E. L. Defect Motifs for Spherical Topologies. *Phys. Rev. B* **2009**, *79*, 224115.
9. Wales, D. J.; Ulker, S. Structure and Dynamics of Spherical Crystals Characterized for the Thomson Problem. *Phys. Rev. B* **2006**, *74*, 212101.
10. Bowick, M. J.; Nelson, D. R.; Travesset, A. Interacting Topological Defects on Frozen Topographies. *Phys. Rev. B* **2000**, *62*, 8738–8751.
11. Irvine, W. T. M.; Vitelli, V.; Chaikin, P. M. Pleats in Crystals on Curved Surfaces. *Nature* **2010**, *468*, 947.
12. Kusumaatmaja, H.; Wales, D. J. Defect Motifs for Constant Mean Curvature Surfaces. *Phys. Rev. Lett.* **2013**, *110*, 165502.
13. Bendito, E.; Bowick, M. J.; Medina, A.; Yao, Z. Crystalline Particle Packings on Constant Mean Curvature (Delaunay) Surfaces. *Phys. Rev. E* **2013**, *88*, 012405.
14. Becker, O. M.; Karplus, M. The Topology of Multidimensional Potential Energy Surfaces: Theory and Application to Peptide Structure and Kinetics. *J. Chem. Phys.* **1997**, *106*, 1495–1515.
15. Wales, D. J.; Miller, M. A.; Walsh, T. R. Archetypal Energy Landscapes. *Nature* **1998**, *394*, 758–760.
16. Fejer, S. N.; Chakrabarti, D.; Wales, D. J. Emergent Complexity from Simple Anisotropic Building Blocks: Shells, Tubes and Spirals. *ACS Nano* **2010**, *4*, 219–228.
17. Wales, D. J. Energy Landscapes: Some New Horizons. *Curr. Opin. Struct. Biol.* **2010**, *20*, 3–10.
18. Irvine, W. T. M.; Bowick, M. J.; Chaikin, P. M. Fractionalization of Interstitials in Curved Colloidal Crystals. *Nat. Mater.* **2012**, *11*, 948–951.
19. Meng, G.; Paulose, J.; Nelson, D. R.; Manoharan, V. N. Elastic Instability of a Crystal Growing on a Curved Surface. *Science* **2014**, *343*, 634–636.
20. Ershov, D.; Sprakel, J.; Appel, J.; Cohen Stuart, M. A.; van der Gucht, J. Capillarity-Induced Ordering of Spherical Colloids on an Interface with Anisotropic Curvature. *Proc. Natl. Acad. Sci. U.S.A.* **2013**, *110*, 9220–9224.